Chem Rep, 2021, 3(1): 195-202
DOI: 10.25082/CR.2021.01.004

RESEARCH ARTICLE

Neuron-like tubule extension of giant polymer vesicles

Eri Yoshida

Department of Applied Chemistry and Life Science, Toyohashi University of Technology, Tempaku-cho, Toyohashi, Aichi 441-8580, Japan

Correspondence to: Eri Yoshida, Department of Applied Chemistry and Life Science, Toyohashi University of Technology, 1-1 Hibarigaoka, Tempaku-cho, Toyohashi, Aichi 441-8580, Japan;
E-mail: yoshida.eri.gu@tut.jp

Received: October 26, 2021;
Accepted: November 25, 2021;
Published: November 26, 2021.

Citation: Yoshida E. Neuron-like tubule extension of giant polymer vesicles. *Chem Rep*, 2021, **3**(1): 195-202. https://doi.org/10.25082/CR.2021.01.004

Abstract: Giant polymer vesicles consisting of amphiphilic diblock copolymers are helpful as artificial biomembrane models based on many similarities in their size, structure, morphological transformation, membrane permeability, *etc*. This paper describes the creation of neuron-like tubule extension employing the polymer vesicles. The polymerization-induced self-assembly was performed in the presence of micron-sized spherical vesicles consisting of poly(methacrylic acid)-*block*-poly(methyl methacrylate-*random*-methacrylic acid), PMAA-*b*-P(MMA-*r*-MAA), through the photo nitroxide-mediated controlled/living radical polymerization (photo-NMP) using 4-methoxy-2,2,6,6-tetramethylpiperidine-1-oxyl (MTEMPO) as the mediator. The photo-NMP of methyl methacrylate (MMA) and methacrylic acid (MAA) was carried out in an aqueous methanol solution (CH_3OH/H_2O = 3/1 *v*/*v*) using poly(methacrylic acid) (PMAA) end-capped with MTEMPO and the spherical vesicles of $PMAA_{141}$-*b*-$P(MMA_{0.831}$-*r*-$MAA_{0.169})_{368}$ with an 11.7 μm diameter. The vesicles projected many processes on their surface during the early stage of the polymerization. As the polymerization progressed, only one or two of the processes extended to thick tubules, accompanied by the slow growth of thin tubules. Further progress of the polymerization elongated the thick tubules and caused branching of the tubules. The tubules had a vesicular structure because cup-like vesicles joined in line were formed during the initial stage of the extension. The polymerization livingness supported the tubule extension based on a linear increase in the molecular weight of the component copolymer and a negligible change in the molecular weight distribution versus the monomer conversion. The spherical vesicles were similar to the neurons in the tubule extension for the initial projection, followed by the elongation and branching. This similarity implies that the neurite extension in the neurons is related to the inherent property of the bilayer membrane.

Keywords: polymer vesicles, tubule extension, cup-like vesicles, neurons, polymerization-induced self-assembly, photo-NMP

1 Introduction

Neurons are the principal cells that perform activities of the brain. They coordinate the functions of many different organs in animal bodies by communicating information to all parts of the body. The neuron transmits an electric impulse generated in its cell body, the soma, by extending the axon formed by projecting the cytoplasmic membrane and delivers the information to another neuron or a glial cell by releasing chemical neurotransmitters from the synapse located at the axon terminal [1, 2]. The neuron and glia receive the neurotransmitters from their synapses on the branch-like dendrites and convey the information to their somata. The neurites of the axon and dendrites extend in the right direction due to the handlike growth cones situated at their growing terminals where the fingerlike filopodia continuously extend and retract to search the direction [3–5]. The components of the neurite membrane are always provided by the neuron itself to extend the neurites, since the neuron contains organelles, including the endoplasmic reticulum and Golgi apparatus [6, 7]. A network of over 10 billion such neurons maintains the functions at the center of the brain.

Giant vesicles in a micron size are significant as artificial biomembrane models for cells and organelles due to similarities in their size and structure [8, 9] In particular, giant polymer vesicles consisting of a poly(methacrylic acid)-*block*-poly(methyl methacrylate-*random*-methacrylic acid) diblock copolymer, PMAA-*b*-P(MMA-*r*-MAA), have found many features in common with the biomembranes based on the morphologies [10], their transformation [11, 12], stimuli-responsive behavior [13, 14], and membrane permeability [15]. These similarities of the polymer vesicles to the biomembranes produced some unique models involved in the biomembranes; for instance, the villi structure using worm-like vesicles vertically aligned [16], the nuclear envelop morphology by perforated vesicles [17], the ion channel by incorporating ionic compounds

into the hydrophobic vesicle core [15], the budding separation of the vesicle membrane using a polyelectrolyte inductor for cytosis [18], and the artificial sterol using the P(MMA-*r*-MAA) segment copolymer [19]. It was found that the polymer vesicles extended tubules from their surface as the neurons extended their neurites. This paper describes the extension of tubules from the surface of the spherical vesicles by polymerization in their hydrophobic cores.

2 Experimental

2.1 Instrumentation

An Ushio UV irradiation system consisting of an optical modulex BA-H502, an illuminator OPM2-502H with a high-illumination lens UI-OP2SL, and a 500W super high-pressure UV lamp USH-500SC2 was used for the polymerization-induced self-assembly by the photo-NMP. ^{1}H NMR measurements were conducted using Jeol ECS400 and ECS500 FT NMR spectrometers. Gel permeation chromatography (GPC) was performed at 40°C using a Tosoh GPC-8020 instrument equipped with a DP-8020 dual pump, a CO-8020 column oven, and a RI-8020 refractometer. Two gel columns of Tosoh TSK-GEL α-M were used with an eluent of *N*,*N*-dimethylformamide containing 30 mM LiBr and 60 mM H_3PO_4. The molecular weight (M_n) and molecular weight distribution (M_w/M_n) were estimated by GPC based on PMAA standards. Field emission scanning electron microscopy (FE-SEM) measurements were performed using a Hitachi SU8000 scanning electron microscope. The vesicles were dried in air and subjected to the FE-SEM measurements at 1.0 kV without any coating.

2.2 Materials

The spherical vesicles previously prepared were used [20]. MAA was purified by distillation under reduced pressure. MMA was passed through a column packed with activated alumina to remove an inhibitor and distilled over calcium hydride. The MMA thus purified were degassed with Ar for 15 min with stirring just before use. MTEMPO was prepared as reported previously [21]. 2,2'-Azobis[2-(2-imidazolin-2-yl)propane] (V-61) and (4-*tert*-butylphenyl)diphenylsulfonium triflate (^{t}BuS) were purchased from Wako Pure Chemical Industries and Sigma-Aldrich, respectively, and used as received. Methanol (MeOH) was refluxed over magnesium with a small amount of iodine for several hours and then distilled. Distilled water purchased from Wako Pure Chemical Industries was purified by distillation. Extremely pure N_2 gas with over 99.9995 vol% purity and Ar gas with over 99.999 vol% purity were purchased from Taiyo Nippon Sanso Corporation.

2.3 Tubule extension from the spherical vesicles

PMAA end-capped with MTEMPO was prepared as reported previously [20]; V-61 (17.1 mg, 0.0683 mmol), MTEMPO (13.5 mg, 0.0725 mmol), ^{t}BuS (18.0 mg, 0.0384 mmol), MAA (3.045 g, 35.4 mmol), and MeOH (6 mL) were placed in a 30-mL test tube joined to a high vacuum valve. The contents were degassed several times using a freeze-pump-thaw cycle and then charged with Ar. The photo-NMP was carried out at room temperature for 11.5 h with irradiation at 9.0 amperes by a reflective light using a mirror with a 500W super high-pressure UV lamp to avoid any thermal polymerization caused by the direct irradiation [22]. MeOH (3.75 mL) degassed by bubbling Ar for 15 min were added to the product under a flow of Ar. After the product was completely dissolved in the MeOH, part of the mixture (ca. 0.2 mL) was withdrawn to determine the MAA conversion. The conversion was 86% by ^{1}H NMR. The solution removed was poured into 50 mL of ether to precipitate the PMAA. The precipitate was collected and dried in vacuo for several hours to obtain the PMAA end-capped with MTEMPO (54.7 mg). The molecular weight and molecular weight distribution of the PMAA were M_n = 27,800 and M_w/M_n = 1.71, respectively, by GPC based on PMAA standards. The degree of polymerization (DP) of the PMAA was calculated to be DP = 319 based on this molecular weight.

The spherical vesicles consisting of $PMAA_{141}$-*b*-$P(MMA_{0.831}$-*r*-$MAA_{0.169})_{368}$ (35.4 mg) were added to a mixed solvent of MeOH (0.4 mL) and water (1.0 mL). The mixture was stirred at room temperature for 2 h in a 30-mL test tube to disperse the vesicles in the solvent. To a suspension of the mixture were added the PMAA solution (2.6 mL containing 0.0193 mmol of the PMAA and 1.29 mmol of the unreacted MAA based on 86% of the MAA conversion), MMA (683mg, 6.82 mmol), and MAA (35.5 mg, 0.413 mmol) under a flow of Ar. The initial molar ratio of the monomers was MMA/MAA = 0.800/0.200. The contents were degassed in vacuo several times by a freeze-pump-thaw cycle and finally charged with Ar. The polymerization was carried out for 4.5 h at room temperature with a 600-rpm stirring speed by irradiation at

8.9 amperes. Part of the resulting dispersion (ca. 0.2 mL) was removed to determine monomer conversions. A mixed solvent of MeOH and water (CH_3OH/H_2O = 3/1 *v/v,* 20 mL) was added to the resulting dispersion to precipitate the aggregates. The aggregates were cleaned by a repeated sedimentation-redispersion process using the solution and stored in a small amount of the mixed solvent.

3 Results and discussion

The polymerization-induced self-assembly was performed in the presence of the micron-sized spherical vesicles in order to extend tubules from their surfaces. The photo-NMP of MMA and MAA was carried out using the PMAA end-capped with MTEMPO and the spherical vesicles consisting of $PMAA_{141}$-*b*-$P(MMA_{0.831}$-*r*-$MAA_{0.169})_{368}$ (M_n = 45,800, M_w/M_n = 1.51 and D_n = 11.7 μm, D_w/D_n = 1.72) [20] in an aqueous methanol solution (CH_3OH/H_2O = 3/1 *v/v*) (Figure 1). The polymerization was initiated outside the spherical vesicles because the PMAA had no hydrophobic chain. As the polymerization progressed, a resulting hydrophobic block chain attached to the PMAA was incorporated into the hydrophobic core of the spherical vesicles. Some of the block chains aggregated into unspecific shapes on the vesicle surface before being incorporated into the hydrophobic core, resulting in the roughness of the surface. In addition, the polymerization without the PMAA produced no tubules and processes.

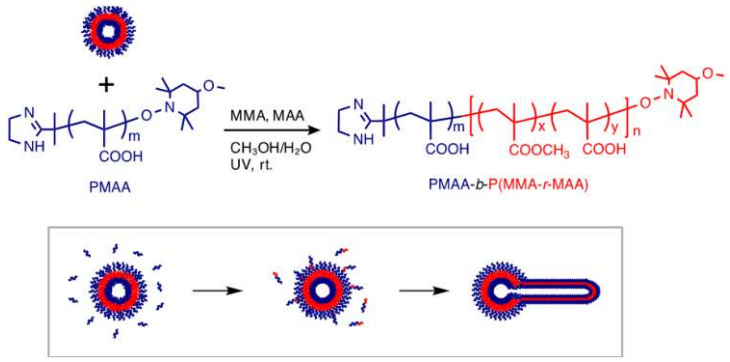

Figure 1 A synthetic scheme of the spherical vesicles to extend the tubules from their surfaces.

FE-SEM observations demonstrated that the spherical vesicles extended tubules from their surfaces (Figure 2). The vesicles projected many processes in their surface during the early stage of the polymerization (Figure 2b and 2c). As the polymerization progressed, only one or two thick tubules extended from the vesicle surface (Figure 2d), accompanied by the slow growth of the thin tubules (Figure 2e). Some tubules consisted of cup-like vesicles joined in line (Figure 2f). The cup-like vesicles produced during the initial stage of the tubule extension indicate that the tubules have a vesicular structure because cup-shaped vesicles were found during the early stage of the worm-like vesicle formation [23]. The tubules were still more elongated by further progress of the polymerization (Figure 2g). The polymerization progress also caused the branching of some tubules (Figure 2h). The tubule extension from the vesicle surface was extremely similar to the axon extension of neurons; the embryonic hippocampal cells extend several short processes during the initial stage. One of the neurites elongates more rapidly than the others to become the axon, while the other processes more slowly grow and branch into the dendrites [24–26]. There is a crucial difference between the spherical vesicles and neurons in the tubule extension. The vesicles extend the tubules by the growth of the copolymer chains in their hydrophobic cores. In contrast, the neurons extend the neurites by supplying the membrane components of the lipids and proteins to the neurites. However, the vesicles and neurons share the feature in that they initially project processes and next choose the processes to extend or branch (Figure 3).

The living nature of the polymerization supported the spherical vesicles to extend the tubules. As shown in Figure 4 concerning the first-order time-conversion plots of the monomers, the polymerization was accelerated during its middle and late stages, indicating that the polymerization progressed within the hydrophobic core of the vesicles. The GPC curves of the resulting copolymers were shifted to the higher side of the molecular weight by the polymerization progress (Figure 5). A linear increase in the molecular weight of the copolymer and a negligible change in the molecular weight distribution versus the MMA conversion proved the living mechanism of the polymerization (Figure 6). This livingness of the polymerization assisted the vesicles in extending the tubules.

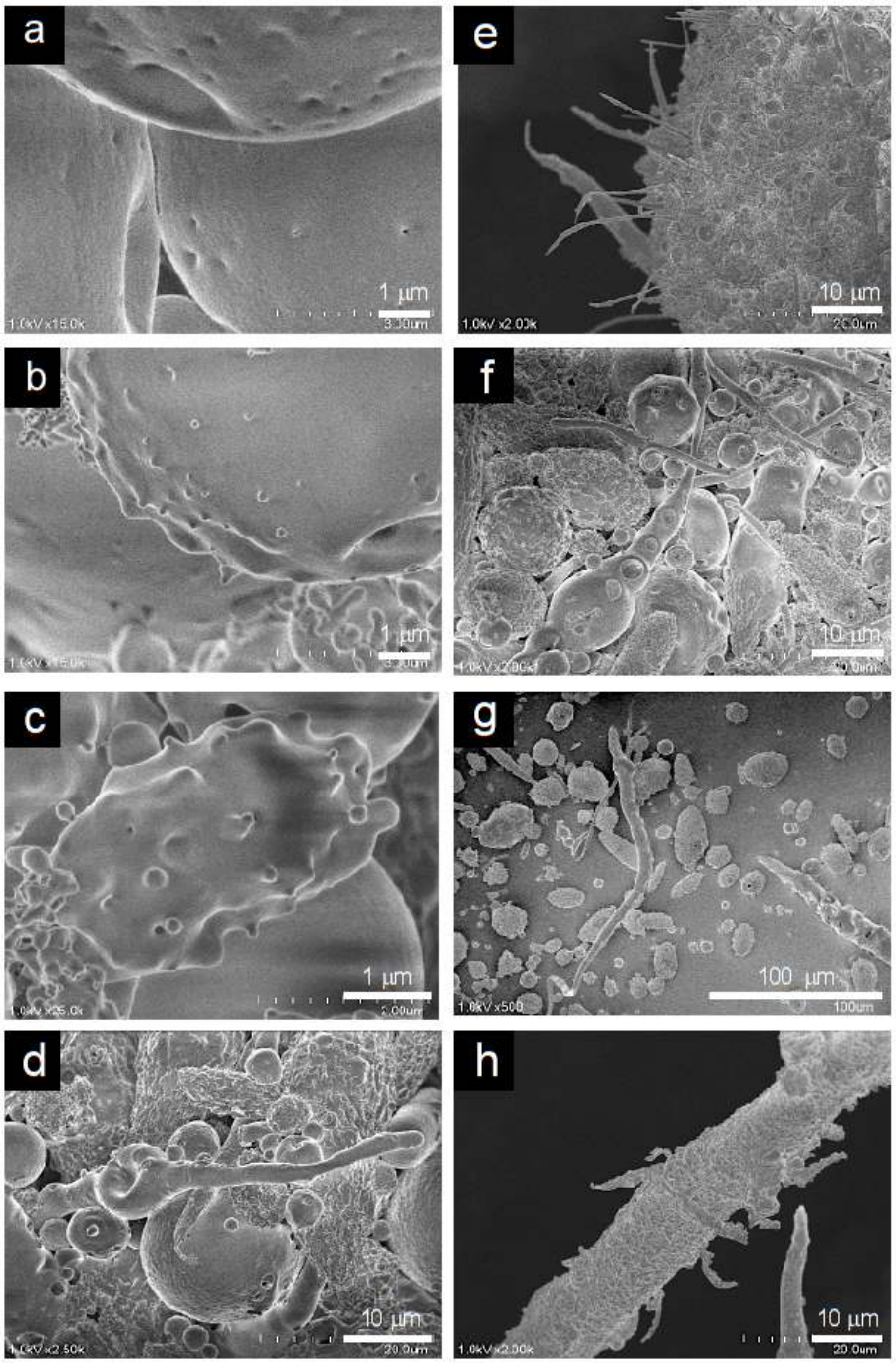

Figure 2 FE-SEM images of the spherical vesicles during the tubule extension by the polymerization-induced self-assembly by the photo-NMP performed for (a) 0 h, (b, c) 1.5 h, (d-f) 3 h, and (g, h) 4.5 h.

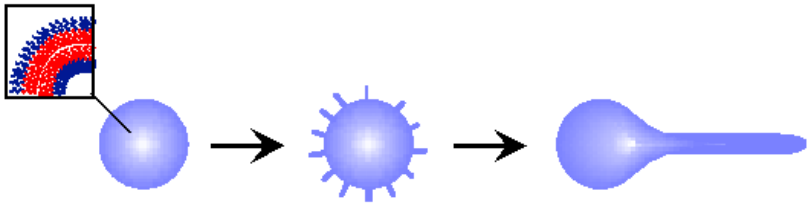

Figure 3 A schematic image of the tubule extension from the vesicle surface.

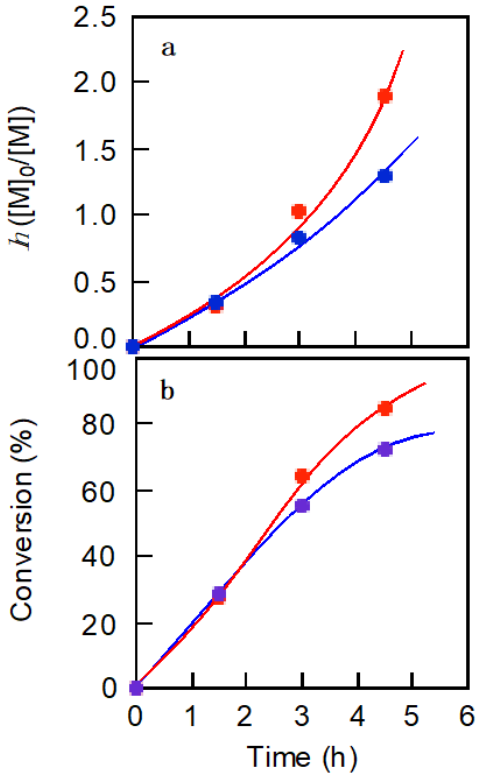

Figure 4 (a) The first-order time-conversion plots and (b) time-conversion plots for the polymerization-induced self-assembly by the photo-NMP of MMA (red) and MAA (blue).

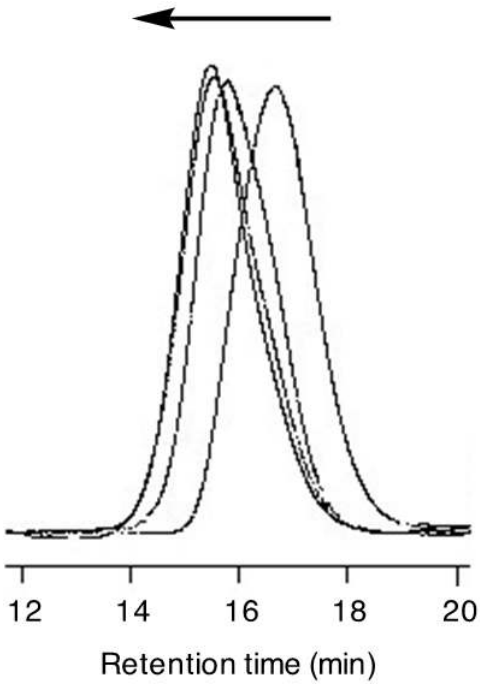

Figure 5 GPC profiles of the PMAA and the resulting diblock copolymers produced by the polymerization-induced self-assembly by the photo-NMP for the polymerization time of 0, 1.5, 3, and 4.5 h from the right.

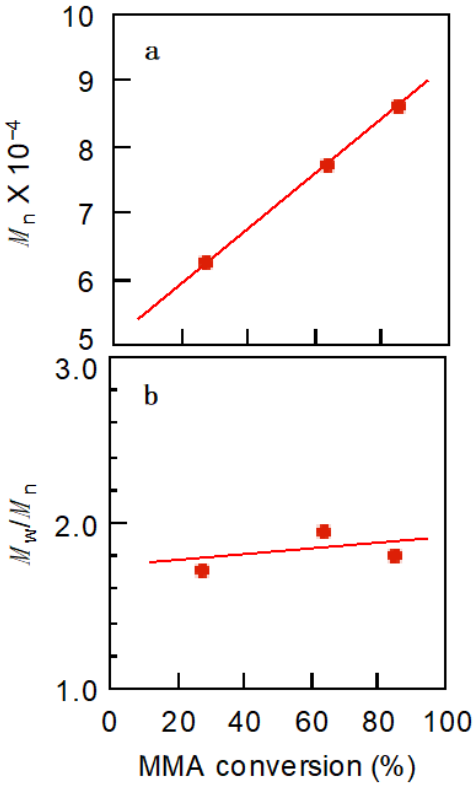

Figure 6 Plots of (a) the molecular weight and (b) molecular weight distribution of the resulting diblock copolymer versus the MMA conversion for the polymerization-induced self-assembly by the photo-NMP.

4 Conclusion

This study demonstrated that the synthetic polymer vesicles performed a neuron-like tubule extension. The vesicles extended tubules from their surface by the polymerization-induced self-assembly using the photo-NMP. The vesicles projected many processes in their surface during the early stage of the polymerization and extended only a few tubules as the polymerization progressed. The tubules had a vesicle structure because the cup-like vesicles were formed during the initial stage of the tubule extension. The polymerization progress further elongated the tubules and branched the tubules. The spherical vesicles were similar to the neurons in the tubule extension for the projection during the initial stage, followed by the tubule elongation and branching, although they had an essential difference in the factor of the extension. This similarity suggests that the neurite extension in the neurons is related to the inherent property of the bilayer membrane.

Conflict of Interest

The author has no conflict of interest in this study.

Acknowledgements

This work was supported by the JSPS Grant-in-Aid for Scientific Research (Grant Number 18K04863).

References

[1] Hall ZW. An Introduction to Molecular Neurobiology. Sinauer Associates, Sunderland, 1992, 1. https://doi.org/10.1212/WNL.19.11.1144

[2] Cosker KE, Courchesne SL and Segal RA. Action in the axon: generation and transport of signaling endosomes. Current Opinion in Neurobiology, 2008, **18**: 270-275. https://doi.org/10.1016/j.conb.2008.08.005

[3] Bentley D and Toroian-Raymond A. Disoriented pathfinding by pioneer neurone growth cones deprived of filopodia by cytochalasin treatment. Nature, 1986, **323**: 712-715. https://doi.org/10.1038/323712a0

[4] Dodd J and Jessell TM. Axon guidance and the patterning of neuronal projections in vertebrates. Science, 1988, **242**: 692-699. https://doi.org/10.1126/science.3055291

[5] Smith SJ. Neuronal cytomechanics: The actin-based motility of growth cones. Science, 1988, **242**: 708-715. https://doi.org/10.1126/science.3055292

[6] Merianda TT, Lin AC, Lam JSY, *et al*. A functional equivalent of endoplasmic reticulum and Golgi in axons for secretion of locally synthesized proteins. Molecular and Cellular Neuroscience, 2009, **40**: 128-142. https://doi.org/10.1016/j.mcn.2008.09.008

[7] Bhattacharyya R, Black SE, Lotlikar MS, *et al*. Axonal generation of amyloid-b from palmitoylated APP in mitochondria associated endoplasmic reticulum membranes. Cell Reports, 2021, **35**: 109134. https://doi.org/10.1016/j.celrep.2021.109134

[8] Elgsaeter A, Stokke BT, Mikkelsen, *et al*. The molecular basis of erythrocyte shape. Science, 1986, **234**: 1217-1223. https://doi.org/10.1126/science.3775380

[9] Frey TG and Mannella CA. The internal structure of mitochondria. Trends in Biochemical Sciences, 2000, **25**(7): 319-324. https://doi.org/10.1016/S0968-0004(00)01609-1

[10] Yoshida E. Fabrication of anastomosed tubular networks developed out of fenestrated sheets through thermo responsiveness of polymer giant vesicles. ChemXpress, 2017, **10**(1): 118. http://www.tsijournals.com/articles/fabrication-of-anastomosed-tubular-networks-developed-out-of-fenestrated-sheets-through-thermo-responsiveness-of-polymer.pdf

[11] Yoshida E. Fission of giant vesicles accompanied by hydrophobic chain growth through polymerization-induced self-assembly. Colloid and Polymer Science, 2014, **292**: 1463-1468. https://doi.org/10.1007/s00396-014-3216-x

[12] Yoshida E. Morphology transformation of micrometer-sized giant vesicles based on physical conditions for photopolymerization-induced self-assembly. Supramolecular Chemistry, 2015, **27**: 274-280. https://doi.org/10.1080/10610278.2014.959014

[13] Yoshida E. PH response behavior of giant vesicles comprised of amphiphilic poly(methacrylic acid)-blockpoly(methyl methacrylate-random-methacrylic acid). Colloid and Polymer Science, 2015, **293**: 649-653. https://doi.org/10.1007/s00396-014-3482-7

[14] Yoshida E. Morphological stability of worm-like vesicles consisting of amphiphilic diblock copolymer against external stress. Chemical Report, 2019, **1**(2): 102-107. https://doi.org/10.25082/CR.2019.02.006

[15] Yoshida E. Enhanced permeability of Rhodamine B into bilayers comprised of amphiphilic random block copolymers by incorporation of ionic segments in the hydrophobic chains. Colloid and Polymer Science, 2015, **293**: 2437-2443. https://doi.org/10.1007/s00396-015-3679-4

[16] Yoshida E. Fabrication of microvillus-like structure by photopolymerization-induced self-assembly of an amphiphilic random block copolymer. Colloid and Polymer Science, 2015, **293**: 1841-1845. https://doi.org/10.1007/s00396-015-3600-1

[17] Yoshida E. Perforated giant vesicles composed of amphiphilic diblock copolymer: New artificial biomembrane model of nuclear envelope. Soft Matter, 2019, **15**: 9849-9857. https://doi.org/10.1039/C9SM01832H

[18] Yoshida E. Morphology transformation of giant vesicles by a polyelectrolyte for an artificial model of a membrane protein for endocytosis. Colloid Surface Science, 2018, **3**: 6-11. https://doi.org/10.11648/j.css.20180301.12

[19] Yoshida E. Morphological changes in polymer giant vesicles by intercalation of a segment copolymer as a sterol model in plasma membrane. Colloid and Polymer Science, 2015, **293**: 1835-1840. https://doi.org/10.1007/s00396-015-3577-9

[20] Yoshida E. Morphology control of giant vesicles by composition of mixed amphiphilic random block copolymers of poly(methacrylic acid)-block-poly(methyl methacrylate-random-methacrylic acid). Colloid and Polymer Science, 2015, **293**: 249-256. https://doi.org/10.1007/s00396-014-3403-9

[21] Miyazawa T, Endo T, Shiihashi S and Ogawara M. Selective oxidation of alcohols by oxoaminium salts (R2N:O+ X-). The Journal of Organic Chemistry, 1985, **50**: 1332-1334. https://doi.org/10.1021/jo00208a047

[22] Yoshida E. Effects of illuminance and heat rays on photo-controlled/living radical polymerization mediated by 4-methoxy-2,2,6,6-tetramethylpiperidine-1-oxyl. ISRN Polymer Science, 2012, 102186. https://doi.org/10.5402/2012/102186

[23] Yoshida E. Worm-like vesicle formation by photo-controlled/living radical polymerization-induced self-assembly of amphiphilic poly(methacrylic acid)-block-poly(methyl methacrylate-random-methacrylic acid). Colloid and Polymer Science, 2016, **294**: 1857-1863. https://doi.org/10.1007/s00396-016-3935-2

[24] Dotti CG and Banker GA. Experimentally induced alteration in the polarity of developing neurons. Nature, 1987, **330**: 254-256.
https://doi.org/10.1038/330254a0

[25] Dotti CG, Sullivan CA and Banker GA. The Establishment of Polarity by Hippocampal Neurons in Culture. The Journal of Neuroscience, 1988, **8**(4): 1454-l488.
https://doi.org/10.1523/JNEUROSCI.08-04-01454.1988

[26] Goslin K and Banker G. Experimental observations on the development of polarity by hippoeampal neurons in culture. The Journal of Cell Biology, 1989, **108**(4): 1507-1516.
https://doi.org/10.1083/jcb.108.4.1507